

Fast gas-ionization wave in a high-power laser beam

V. I. Fisher

Astronomic Observatory of the Odessa State University

(Submitted 12 February 1980)

Zh. Eksp. Teor. Fiz. 79, 2142–2151 (December 1980)

The transport of the absorption zone of laser radiation along the beam is considered. It is shown that at sufficiently high laser intensity, $q_0 > \bar{q}$, the wave-propagation regime differs in principle from the known regimes [Yu. P. Raizer, *Laser Induced Discharge Phenomena*, Consult. Bureau Chap. 6; *Sov. Phys. JETP* 21, 1009 (1965)]. In particular, the plasma temperature T^* behind the wave front decreases with increasing q_0 , and the wave velocity $D(q_0)$ increases more rapidly than a linear function. The structure and regularities of the propagation of the ionization wave are determined.

PACS numbers: 52.40.Db

There are four known regimes of the transport of the absorption zone of laser radiation along the beam: breakdown, optical detonation, radiation, and heat conduction.^{1,2} Theoretical and experimental investigations of these regimes¹⁻¹⁰ show that the dependence of the front velocity D on the laser-radiation intensity q_0 is weaker than linear:

$$D \sim q_0^s, \quad 1/3 < s < 1. \quad (1)$$

The experimentally observed relation $D \sim q_0^{3.5-2}$ offers evidence of the existence of an uninvestigated "fast" regime of front propagation. We shall call this arbitrarily the fast-ionization-wave (FIW) regime and calculate the threshold of the regime and the structure and regularities of the wave propagation.

Streak photographs of the ionization waves show that at a weak $q_0(t)$ dependence the propagation of the front of the wave rapidly becomes stationary. We use as an example in our calculations a plane stationary wave in hydrogen, inasmuch as the cross sections of the elementary process in this gas have been most fully investigated.

RADIATION TRANSPORT

We assume that the intensity of the thermal radiation within the cross section of a cylindrical optical channel differ little from the value calculated for the channel axis (see Figs. 5 and 6 of Ref. 2):

$$I_\nu(\Omega, x, r < R) \approx I_\nu(\Omega, x, 0).$$

In this case the propagation direction Ω is characterized by the angle ϑ between the vector Ω and the channel axis x ; R is the radius of the beam,

$$I_\nu(x, \Omega) = I_\nu(x, \vartheta),$$

and the radiation-transport equation can be represented in the form

$$\cos \vartheta \frac{dI_\nu}{dx} = \kappa_\nu (I_{\nu, \text{eq}} - I_\nu). \quad (2)$$

Here $I_{\nu, \text{eq}}$ is the intensity of the equilibrium radiation, and κ_ν is the absorption coefficient.

The radiation of the plasma from behind the front ionizes the atoms ahead of the front and heats the electron gas. Let Q_e and $\kappa_e^0 q_0$ be the energy released when the electrons are heated by thermal and laser radiation, respectively. It can be shown that

$$\delta = \frac{Q_e}{\kappa_e^0 q_0} < 10^{-25} \frac{\omega^2}{q_0} T_{e,0} T^*.$$

The temperatures are expressed here in electron volts and q_0 in W/cm², ω is the laser frequency, and $T_{e,0}$ at T^* are the electron temperatures ahead and behind the FIW front. The threshold \bar{q} of the FIW regime in hydrogen, for neodymium-laser radiation, is 8 GW/cm², i.e., $q_0 > 8$ GW/cm², and the plasma temperature T^* in all the calculations did not exceed 15 eV. We obtain $\delta < 10^{-3}$. Thus, the heating of the electron gas in the FIW regime is due to the laser radiation.

The role of thermal radiation of the plasma, which is important for the FIW regime, reduces to ionization of the gas,¹⁾ i.e., to ascertain the properties of the FIW Eq. (2) need be solved only for the hard part of the spectrum, $h\nu > I_H$.

The photoionization of the unexcited hydrogen atom is described by the spectral coefficient of the free-bound absorption¹²

$$\kappa_\nu^{\text{ph}} = \frac{32\pi^2 Z_i^2 e^6}{3^3 h^3 c \nu^3} N I_H = 771 \left(\frac{N}{10^{20}} \right) \left(\frac{I_H}{h\nu} \right)^3 \text{cm}^{-1}; \quad h\nu > I_H. \quad (3)$$

Here N is the number of atoms per cm³ and I_H is the ionization potential of hydrogen.

The absorption of the laser and thermal radiations by free electrons in elastic collisions with ions and atoms describes the spectral absorption coefficient corrected for stimulated emission:

$$\kappa_\omega = \frac{4\pi\sigma_\omega}{cn_\omega} \frac{T_e}{h\omega} \left(1 - \exp\left(-\frac{h\omega}{T_e}\right) \right), \quad \omega = 2\pi\nu. \quad (4)$$

Here σ_ω is the conductivity of the plasma and n_ω is the refractive index;

$$\sigma_\omega = \frac{e^2 n}{m} \frac{\nu_c}{\omega^2 + \nu_c^2}, \quad n_\omega^2 = 1 - \frac{\omega_{e0}^2}{\omega^2 + \nu_c^2}, \quad \omega_{e0}^2 = \frac{4\pi e^2 n}{m},$$

$$\left(\frac{2\pi\sigma_\omega}{\omega} \right)^2 \ll 1, \quad \left(\frac{2\pi\sigma_\omega}{\nu_c} \right)^2 \ll 1,$$

ν_c is the frequency of the elastic collisions of the electrons with the ions and atoms.

We discuss now the character of the variation of the absorption coefficient in the fast ionization wave. We introduce a coordinate system connected with the front of the FIW. Let, for the sake of argument, the wave propagate in the positive x direction. The FIW regime is not connected with the hydrodynamic transport and is a superdetonation regime. The ionization of the gas

in the front of the wave is not accompanied by a change of density, and noticeable expansion of the plasma sets in at a distance $|x| > R$ behind the wave front. From among the thermodynamic variables, the only one that influences the coefficient κ_v^{ph} is N , therefore ahead of the absorption front (up to $z \sim 0.1$, where z is the degree of ionization) the coefficient κ_v^{ph} is independent of the coordinate:

$$\kappa_v^{\text{ph}}(x > l_{\text{fr}}) = \kappa_v^{\text{ph}}(l_{\text{fr}}) = \kappa_v^{\text{ph}}.$$

In a narrow absorption-wavefront l_{fr} , the coefficient κ_v^{ph} decreases by a factor $(1 - z^*)^{-1}$, and assumes a new (coordinate-independent) value

$$\kappa_v^{\text{ph}}(x < -l_{\text{fr}}) = (1 - z^*) \kappa_v^{\text{ph}}(l_{\text{fr}}) = \kappa_v^{\text{ph}*}.$$

The asterisk marks the variables behind the front of the FIW ($-R < x < -l_{\text{fr}}$), i.e., after the absorption of the laser radiation but before the start of the plasma expansion.

The coefficient of the bound-free absorption κ_v^{ph} decreases abruptly in a plasma layer of thickness $\sim l_{\text{fr}}$; the bremsstrahlung coefficient κ_v^{e} $\sim z$, on the contrary, increases rapidly in this layer. Ahead of the front, $\kappa_v^{\text{ph}} \gg \kappa_v^{\text{e}}$, therefore the combined absorption coefficient in the hard part of the spectrum can be represented in the form

$$\kappa_v(x, h\nu > I_{\text{H}}) \approx \begin{cases} \kappa_v^{\text{ph}}, & x > 0 \\ \kappa_v^{\text{ph}*} + \kappa_v^{\text{e}}, & x < 0 \end{cases} \quad (5)$$

The photons $h\nu > I_{\text{H}}$ ionize some of the atoms of the cold gas relatively far ahead of the front. The free electrons produced by photoionization within the limits of the optical channel generate an electron avalanche in the next gas layer ahead of the front, if the intensity of the laser radiation is high enough, $q_0 > \bar{q}$. More accurately speaking, the gas ionization rate \dot{n} consists of the photoionization rate \dot{n}_{ph} and of the rate \dot{n}_{e} of ionization by electron impact:

$$\dot{n} = \dot{n}_{\text{e}} + \dot{n}_{\text{ph}}. \quad (6)$$

Calculations performed for a number of typical combinations of experimental parameters show that the condition $\dot{n}_{\text{ph}} \gg \dot{n}_{\text{e}}$ is satisfied only during the initial stage of the ionization of the next gas layer. Further development of the avalanche takes place at a relation $\dot{n}_{\text{ph}} \ll \dot{n}_{\text{e}}$ if $q_0 > \bar{q}$ (see Fig. 4 below). The condition $\dot{n}_{\text{ph}} \gg \dot{n}_{\text{e}}$ is satisfied at a distance λ from the absorption-wavefront which is large compared with the width of the front l_{fr} . In the calculations performed, $\lambda/l_{\text{fr}} \sim 20-100$. This circumstance simplifies substantially the solution of Eq. (2), since the true profile of the coefficient $\kappa_v(x, h\nu > I)$ differs from the steplike profile (5) only in a narrow band $|x| < l_{\text{fr}}$. Inasmuch as the photoionization is substantial only over a distance $x \sim \lambda \gg l_{\text{fr}}$ from the front, the steplike approximation (5) introduces a small error in the calculation of the sum (6).

The thermal radiation that enters into the zone of the priming ionization from behind the front is emitted principally by a cylindrical volume of radius R and height $H \approx R$. Since the FIW regime is superdetonational and $R \gg l_{\text{fr}}$, we can regard the density and temperature of the plasma within this volume as constants, in analogy with Refs. 1 and 2.

For a medium with an absorption coefficient (5), the solution of Eq. (2) is

$$I_v(x, \vartheta) = I_{\nu \text{eq}} \left(1 - \exp\{-\kappa_v L(\vartheta)\} \right) \exp\left\{-\frac{\kappa_v^{\text{e}} x}{\cos \vartheta}\right\} + I_{\nu \text{eq}}^0 \left(1 - \exp\left\{-\frac{\kappa_v^{\text{e}} x}{\cos \vartheta}\right\} \right). \quad (7)$$

Here $L(\vartheta)$ is the length of the "tube" radiating at an angle ϑ :

$$L(\vartheta) = \begin{cases} H/\cos \vartheta, & 0 < \vartheta < \vartheta_1 = \arctg(R/[H+x]) \\ R/\sin \vartheta - x/\cos \vartheta, & \vartheta_1 < \vartheta < \vartheta_2 = \arctg(R/x) \end{cases} \quad (8)$$

$$I_{\nu \text{eq}}^0 = I_{\nu \text{eq}}(T_e). \quad (9)$$

Ahead of the absorption-wavefront the atoms and electrons have substantially different temperatures, $T_0 \ll 1$ eV and $T_{e,0} > 1$ eV. This raises the question of which temperature to use in the calculation of the intensity $I_{\nu \text{eq}}^0$ of the equilibrium radiation of a two-temperature system.

The answer can be obtained by the following reasoning. The emissivity of the plasma is $j_v \sim nm_i$. If the degree of ionization is at equilibrium, $z = z_{\text{eq}}$, then $nm_i \sim \exp(-I/T_e)$ and, in accordance with Kirchhoff's law we have $I_{\nu \text{eq}} \sim \exp(-I/T_e)$, i.e., $I_{\nu \text{eq}} z_{\text{eq}} = I_{\nu \text{eq}}(T_e)$. Ahead of the absorption-wavefront, the degree of ionization is lower than the equilibrium value by several orders of magnitude, so that also

$$j_v/\kappa_v = I_{\nu \text{eq}}(z < z_p) \ll I_{\nu \text{eq}}(T_e),$$

Therefore the intensity of the equilibrium radiation was calculated using the temperature of the atoms:

$$I_{\nu \text{eq}}^0 = I_{\nu \text{eq}}(T_0). \quad (10)$$

The absorption of the laser radiation is described by the equation

$$dq/dx = \kappa_v q \quad (11)$$

with the absorption coefficient (4).

IONIZATION KINETICS

The rate of photoionization of the atom by the thermal radiation is

$$\dot{n}_{\text{ph}} = 2\pi \int_0^{\vartheta_2(x)} \sin \vartheta d\vartheta \int_{\lambda}^{\infty} \frac{\kappa_v^{\text{ph}}(x) I_v(x, \vartheta)}{h\nu} d\nu. \quad (12)$$

At laser-radiation intensity $q_0 \sim (10-1000)$ GW/cm², the average electron energy in the avalanche is $\bar{\varepsilon} \sim (1-5)$ eV. The ratio of the probabilities of excitation and ionization of an atom by electron impact is

$$f(\bar{\varepsilon}) = \frac{\langle \sigma_{\text{ea}}^* \nu_e \rangle}{\langle \sigma_{\text{ia}}^* \nu_e \rangle} \sim 10-100. \quad (13)$$

Here σ_{ea}^* is the combined cross section for the excitation of atomic levels by electron impact, and the angle brackets denote averaging over the Maxwellian distribution. Thus, excitation of an atom is much more frequent than ionization. The excited atoms are rapidly ionized by the laser radiation. Thus, e.g., the probability of ionization of the 2S level of the hydrogen atom by two photons of a ruby laser is $w \sim 10^4$ sec⁻¹ at $q_0 = 10$ GW/cm²,¹³ i.e., the photoionization of excited levels by laser radiation can be regarded as instantaneous, since the photoionization time w^{-1} is much shorter than all the

relaxation times involved in the problem.

The effective frequency of the ionization of the atoms by electron impact consists thus of the frequency of the direct ionization and the frequency of the level excitation:

$$v_z = v_i + v_{ex} = N \langle \sigma_{ca} v_e \rangle + N \langle \sigma_{ca} v_e \rangle. \quad (14)$$

To check on this statement, Phelps¹⁴ calculated the avalanche development time in argon and compared the results with experiment. The comparison has shown that the assumption of instantaneous photoionization of the excited levels corresponds more to reality than the assumption of direct ionization by electron impact.

The first electrons appear in the light channel as a result of the photoeffect at a distance λ ahead of the front. It can be shown that the main contribution to the production of the priming ionization are made by photons with $h\nu \sim 30$ eV, therefore the initial electron energy amounts on the average to $\bar{\epsilon}_{ph} \sim 20$ eV. The probabilities of elastic and inelastic collisions of electrons of this energy are close in value. Therefore the energy lost in elastic collision with the atom is low, $\Delta\epsilon \sim m\epsilon/M$, and the electron ionizes or excites the atom after several elastic collisions. The excited atom is ionized by the laser radiation. The loss of the photoelectron energy in inelastic collisions exhausts practically completely its initial energy reserve, and the remainder is consumed in elastic collisions. Thus, practically each photoionization act yields two free electrons. The time of ionization of the atom by the photoelectron ($\bar{\tau}_{ph} \approx 20$ eV) is shorter by two orders of magnitude than the time necessary for the appearance of a new generation of electrons in the avalanche so that the doubling of the photoelectron can be regarded as instantaneous.

Summarizing the statements made above concerning the ionization mechanisms, we can write the ionization-kinetics equation in the form

$$\dot{n} = 2a_{ph}N + \alpha Nn - 2b_{ph}n^2 - \beta n^3. \quad (15)$$

The photoionization probability of the atom a_{ph} is calculated from formula (12), $a_{ph} = N^{-1} \dot{n}_{ph}$, and the rate of impact ionization is $\alpha Nn = n\nu_{\Sigma}$.

Recombination comes into play only during the concluding stage of the avalanche development, when a degree of ionization $z \sim z_{eq}/10$ is reached. The recombination rate is calculated in the usual manner from the equilibrium constant and the ionization rate¹²:

$$b_{ph} = a_{ph}/k_{eq}; \quad \beta = \alpha/k_{eq}.$$

HEATING OF ELECTRONS AND ATOMS

We consider the motion of a planar layer of gas towards the front of an FIW. Neglecting the small change of the thermodynamic properties of the gas within the limits of an arbitrarily layer, we write down the energy conservation law for the electron subsystem:

$$\epsilon_c = \nu_{ex} q - \frac{2m}{M} \nu_c n \frac{3}{2} (T_e - T) - I \dot{n}. \quad (16)$$

The electron energy is consumed in heating, excitation, and ionization of the atoms, I is the average energy consumed in formation of one electron, and is close to

the potential of the first excited level (13).

The rate of ionization and excitation by electron impact is

$$\dot{n}_e = \alpha Nn - \beta n^3.$$

The volume density of the internal energy of the electron subsystem is²⁾

$$\epsilon_e = \frac{3}{2} n T_e. \quad (17)$$

The atoms and ions form a second subsystem, which is heated in elastic collisions by energy transfer from the electron gas:

$$\dot{T} = \frac{2m}{M} \frac{n}{N} \nu_c (T_e - T). \quad (18)$$

We eliminate ϵ_e and q from (16) with the aid of (11) and (17). Adding the obtained equation to (18) multiplied by $3N/2$, and integrating from $x \leq -l_{fr}$ to $x \rightarrow \infty$, we obtain the energy conservation law:

$$q_0 = N_0 D [\frac{3}{2} T_e^* (1+z^*) + I z^* - \frac{3}{2} T_0]. \quad (19)$$

Equation (16) is linear in n at $z \ll z_{eq}$, therefore the growth of the degree of ionization in the course of motion of a selected layer of gas takes place at constant electron temperature $T_{e,0}(q_0)$. Only attainment of an ionization degree comparable with the equilibrium value at the given temperature can decrease the energy lost by the electron assembly to ionization of the atoms and create conditions for an increase of T_e . Starting with this instant, the ionization "follows" the temperature growth.

Since the electron temperature in the avalanche is constant, it can be determined from (16) by equating its right-hand side to zero. Neglecting recombination, we write $\dot{n}_e \approx \nu_{\Sigma} n$, so that we can represent (16) in the form

$$v_i + v_{ex} = \nu_c \left(\frac{4\pi e^2}{cm} \frac{q_0}{\omega^2 + \nu_c^2} - \frac{3m}{M} T_{e,0} \right) \left(I + \frac{3}{2} T_{e,0} \right)^{-1}. \quad (20)$$

Substituting the explicit expressions for the collision frequencies^{12, 15, 16}

$$\begin{aligned} v_i &= \pi a_0^2 N \bar{\nu}_e \exp(-I/T_e), \quad \bar{\nu}_e = (8T_e/\pi m)^{1/2}, \\ v_{ex} &= 2.5 \cdot 10^{-16} N \bar{\nu}_e \exp(-I/T_e), \\ v_o &= 2.2 \cdot 10^{-7} N + 2(2\pi/m)^{1/2} e^4 \Lambda n T_e^{-3/2} \end{aligned} \quad (21)$$

in Eq. (20), we obtain the explicit relation $q = q_0(T_{e,0})$. Inverting this relation, we obtain the dependence of the electron temperature in the avalanche ahead of the front on the laser-radiation intensity $T_{e,0}(q_0)$. Here a_0 is the Bohr radius and Λ is the Coulomb logarithm.

THE SOLUTION

The quantity λ was defined above as the distance between the front of the absorption wave and the gas layer (perpendicular to the light-channel axis) in which the first priming electrons are produced, i.e., the ionization rate has a certain physically small value. To make the further calculations specific, we assume as the minimum ionization rate $\dot{n}_m = \dot{n}_{ph}^{\min}$ such that one electron is produced in a volume of 10^{-6} cm³ during the time of passage of the wave through the layer of 1 μ m, i.e., $\Delta t = 10^{-4}$ cm/D. Here D is the wave velocity in cm/sec:

$$\dot{n}_m = 10^{12} D \text{ [cm}^{-3}\text{sec}^{-1}\text{]}. \quad (22)$$

The choice of the numerical value is quite arbitrary, but reasonable in order of magnitude. It must be emphasized that the quantity n_m is introduced only to determine the initial coordinate λ , from which the integration of the system (11), (15), (16), and (18) begins, and the ionization wave starts where at least one electron is produced during the characteristic time in the characteristic volume. The dependence of the solution on the value of n_m is very weak. Thus, e.g., at $R=1$ mm, $N_0=10^{20}$ cm $^{-3}$, and $q_0=30$ GW/cm 2 an increase of n_m by two orders of magnitude compared with (22) decreases the wave velocity from 895 to 733 km/sec.

The laws governing the propagation of the FIW can be easily determined by numerically integrating the system (11), (15), (16), (18). From the intensity of the thermal radiation (7) one calculates the atom photoionization rate (12). The initial coordinate λ is determined from the condition (22). At this point, we specify the initial values

$$q=q_0, z=0, T_{e,0}=T_e(q_0), T_0=0.5 \text{ eV.}$$

The quantity $T_e(q_0)$ is calculated from (20) and (21). To simplify the calculations, the gas was assumed to be atomic,³ and therefore we assumed $T_0=0.5$ eV. The connection between the initial and final states is ensured by the energy conservation law and by the Saha equation (equilibrium of ionization in the final state), but one equation is insufficient to find the three quantities D , T^* , and z^* . In problems on the structure of optical detonation waves, the system is made closed by the Jouguet condition. In the problem of the structure of the FIW, the flux of the thermal radiation was calculated under the assumption that the "step" of the absorption coefficient (5) is located at $x=0$, and therefore the solution of the system of differential equations—the structure of the wave—should satisfy this requirement.

The wave velocity D is an eigenvalue of the equations that describe the structure of the waves. The same problem of finding W arises, e.g., in the theory of combustion or in the theory of ionizing shock waves in a magnetic field. The condition for the determination of an eigenvalue is, in the standard formulation, the passage of the integral curve through two singular points corresponding to equilibrium state ahead of and behind the wave. In the considered problem, it turned out to be more convenient in practice, in the calculation of the leading radiation to choose in explicit fashion the origin (the initial equations are invariant to the shift $x \rightarrow x + x_0$). The solution of the equations for the structure at the chosen origin satisfy the boundary condition at a single value of D . Integrating this system of equations for different values of D , we choose as the wave structure the solution closest to (5), namely, the one satisfying the requirement

$$x(0) = [x(-R) + x(\lambda)]/2. \quad (23)$$

An arbitrary change of the wave velocity by 1% compared with the solution shifts the step by $\Delta x \gg l_{pr}$, thus attesting to the high accuracy with which the solutions are obtained from the condition (23).

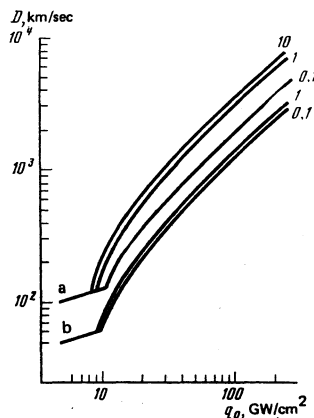


FIG. 1. The transition from the optical detonation regime ($\gamma=5/3$) to the FIW regime in hydrogen. Neodymium laser. Gas density ahead of the front $N_0=10^{20}$ cm $^{-3}$ (a) and 9×10^{20} cm $^{-3}$ (b). The numbers indicate the radius of the beam in millimeters.

DISCUSSION OF RESULTS

The most notable feature of the FIW regime is the unusually strong (compared with Refs. 1–10) $D(q_0)$ dependence observed for argon and xenon in an experiment with a high-power CO $_2$ laser.¹¹ A similar dependence is obtained from calculations made for hydrogen, Fig. 1. The threshold of the transition from the optical-detonation regime ($\gamma=5/3$) to the FIW regime amounts to $\bar{q}=(8-10)$ GW/cm 2 and depends little on N_0 and R . The strong $D(q_0)$ dependence for the FIW regime near the threshold makes the threshold practically independent of the course of the $D(q_0)$ curve at $q_0 < \bar{q}$. Near the threshold we have $D \sim q_0^{3-4}$ in analogy with Ref. 11, and at $q_0 \gg \bar{q}$ we have $D \sim q_0^{1+\epsilon}$, where $0 < \epsilon(q_0) \ll 1$ is a decreasing function. A decrease of the exponent with increasing q_0 was observed also in Ref. 11.

A typical FIW structure is shown in Fig. 2. In this calculation, the wave velocity is 236 km/sec, the plasma temperature behind the front is 2.35 eV; the equilibrium degree of ionization is $z_{eq}^* = 0.174$; $\lambda = 0.2$ mm; $l_{pr} \approx 5$ μ m; $H=R=1$ mm. The profile of the absorption coefficient is given for $h\nu=21.5$ eV. The relation $\kappa_\nu \sim \nu^{-3}$ at $h\nu \gg T$ makes it possible to recalculate this profile for other frequencies. The appreciable value of the absorption coefficient behind the front κ_ν^* is explained by the relatively low temperature T^* in this calculation (see Fig. 3), by the low ionization $z_{eq}^*(T^*)$,

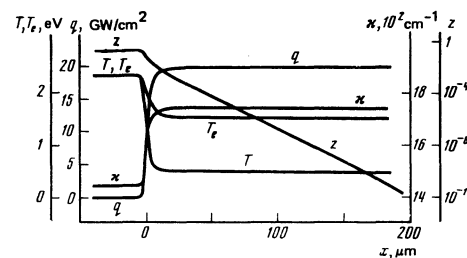


FIG. 2. Structure of FIW in hydrogen. $N_0=9 \times 10^{20}$ cm $^{-3}$. Neodymium-laser radiation intensity $q_0=20$ GW/cm 2 , $R=H=1$ mm.

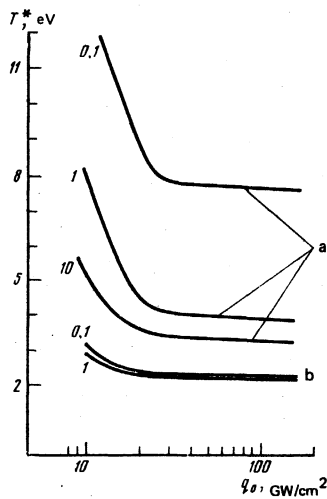


FIG. 3. Plasma temperature behind the front of an FIW. The notation is the same as in Fig. 1.

and consequently by the low photoabsorption, see (3)–(5). Figure 4a allows us to compare the rate of avalanche ionization with the rate of the photoionization in the waves shown in Fig. 2. The time is reckoned “backwards” from the instant that the wavefront is reached by the considered gas layer. The ionization of the cold-gas layer takes place in this calculation at $\tau^* \approx 0.9$ nsec. A comparison of the quantities

$$Z_a = N_0^{-1} \int_{-\tau^*}^0 \dot{n}_e dt, \quad Z_{ph} = N_0^{-1} \int_{-\tau^*}^0 \dot{n}_{ph} dt$$

shows that the role of photoionization in the wave reduces to a “triggering” of the electron avalanche. The ratio $Z_{ph}(0)/Z_a(0)$ increases gradually with decreasing q_0 , i.e., with weakening of the avalanche mechanism, but even near the threshold of the transition to the optical detonation regime (Fig. 4b) the rate of photoionization is lower by one order of magnitude than the rate of avalanche ionization.

The functions $D(q_0)$ and $T^*(q_0)$ are connected by the energy conservation law (19). In the FIW regime, $s(q_0) > 1$ in a ratio $D \sim q_0^3$, therefore an increase of q_0 is inevitably accompanied by a decrease of $T^*(q_0)$ (Fig. 3). The unusual form of the $T^*(q_0)$ dependence is also a distinguishing feature of the FIW regime, while in the remaining regime the function $T^*(q_0)$ increases monotonically. Such a substantial difference of this relation from the results of Refs. 1–10 is quite easy to explain: in the FIW regime, the increase of \dot{n}_e with increasing $T_{e,0}(q_0)$ is much more substantial than the decrease of \dot{n}_{ph} due to the decrease of $T^*(q_0)$.

In conclusion, we discuss briefly the influence of the parameters R and N_0 on the regularities of the FIW regime. At high pressure of the cold gas ahead of the front, the plasma temperature T^* behind the front is low, the ionization of the gas is weak, $z^* \sim 0.2$ – 0.3 , and already at $R = 0.1$ mm the optical thickness of the luminous layer is large practically in the entire ionizing part of the plasma-emission spectrum. The spectrum and intensity of the radiation are thus close to equilibrium at T^* , therefore an increase of the radius of the

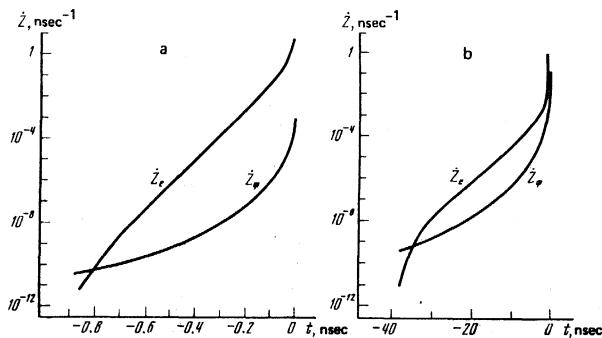


FIG. 4. Comparison of the rates of avalanche ionization and photoionization in an FIW propagating in hydrogen opposite to the radiation of a neodymium laser: a) $q_0 = 20$ GW/cm², $N_0 = 9 \times 10^{20}$ cm⁻³, $R = 1$ mm; b) $q_0 = 10$ GW/cm², $N_0 = 10^{20}$ cm⁻³, $R = 1$ mm.

beam has practically no influence on the FIW parameters. At a lower gas density ahead of the front ($N_0 = 10^{20}$ cm⁻³) the spectrum and intensity of the plasma radiation depend substantially on the beam radius (via the optical thickness of the hot zone), and therefore the parameters of the FIB also depend on R .

The discovery of the FIW regime has a strong influence on the choice of the optimal regime of compression of gas targets for laser-driven thermonuclear fusion. At $q_0 > \bar{q}$ the absorption zone of the laser radiation is coupled to the front of the optical-detonation wave for a relatively short time—the formation of the luminous plasma layer causes detachment of the absorption zone is coupled with the FIW front. The growth of q_0 is accompanied by a growth of T^* only at $q_0 < \bar{q}$, after which the temperature decreases sharply, thus decreasing the momentum transfer to the surface of the shell.

The author thanks S. I. Anisimov and P. P. Pashinin for helpful discussions.

¹It is here that the difference between the FIW regime and the radiation regime (RR) manifests itself.^{1,2} In the RR the plasma should ensure by its thermal radiation the transport of the front—to increase the velocity it is necessary to increase T^* . But then the energy conservation law calls for a decrease of the function $D(q_0)/q_0$ with increasing q_0 , from which it follows that $s < 1$ in (1) for the RR.

²In the performed calculations the contribution of the Coulomb interaction to the internal energy is small. The plasma is a nondegenerate ideal gas.

³Allowance for the kinetics of the dissociation and for the collisions of the electrons with the molecules complicates somewhat the calculations, but does not change the character of the solution.

¹Yu. P. Raizer, *Laser Induced Discharge Phenomena*, Consultants, 1974, Chap. 6.

²Yu. P. Raizer, *Zh. Eksp. Teor. Fiz.* 48, 1508 (1965) [*Sov. Phys. JETP* 21, 1009 (1965)].

³S. I. Anisimov, M. F. Ivanov, P. P. Pashinin, and A. M. Prokhorov, *Pis'ma Zh. Eksp. Teor. Fiz.* 22, 343 (1975) [*JETP Lett.* 22, 161 (1975)].

⁴A. M. Prokhorov, S. I. Anisimov, and P. P. Pashinin, *Usp. Fiz. Nauk* 119, 401 (1976) [*Sov. Phys. Usp.* 19, 547 (1976)].

⁵V. V. Korobkin, S. L. Mandel'shtam, P. P. Pashinin, A. V.

- Prokhindeev, A. M. Prokhorov, N. K. Sukhodrev, and M. Ya. Shchelev, *Zh. Eksp. Teor. Fiz.* 53, 116 (1967) [*Sov. Phys. JETP* 26, 79 (1968)].
- ⁶V. A. Gal'bert and M. F. Ivanov, Preprint ITF AN SSSR, 1979.
- ⁷I. E. Markovich, L. V. Nemchinov, A. I. Petrukhin, Yu. E. Pleshnikov, and V. A. Rybakov, *Pis'ma Zh. Tekh. Fiz.* 3, 101 (1977) [*Sov. Tech. Phys. Lett.* 3, 40 (1977)].
- ⁸I. E. Markovich, I. V. Nenchinov, A. I. Petrukhin, Yu. E. Pleshnikov, and V. A. Rybakov, *Fiz. Plazmy* 5, 1003 (1979) [*Sov. J. Plasma Phys.* 5, 560 (1979)].
- ⁹V. I. Bergel'son, T. V. Loseva, I. V. Nemchinov, and T. I. Orlova, *ibid.* 1, 912 (1975) [1, 498 (1975)].
- ¹⁰I. E. Poyurovskaya and V. I. Fisher, *Zh. Tekh. Fiz.* 48, 177 (1978) [*Sov. Phys. Tech. Phys.* 23, 103 (1978)].
- ¹¹V. A. Boiko, V. A. Danilychev, B. N. Duvanov, V. D. Zvorykin, and I. V. Kholin, *Kvant. Elektron. (Moscow)* 5, 216 (1978) [*Sov. J. Quantum Electron.* 8, 134 (1978)].
- ¹²Ya. B. Zel'dovich and Yu. P. Raizer, *Fizika udarnykh voln (Physics of Shock Waves)*, Nauka, 1966.
- ¹³H. Webb and A. Gold, transl. in: *Deistvie lazernogo izlucheniya (Action of Laser Radiation)*, Mir, 1968, p. 85.
- ¹⁴A. Phelps, *ibid.* p. 23.
- ¹⁵V. I. Ginzburg, *Rasprostranenie elektromagnitnykh voln v plazme (Propagation of Electromagnetic Waves in Plasma)*, Nauka, 1967, p. 79 [Pergamon].
- ¹⁶S. I. Anisimov and V. I. Fisher, *Zh. Tekh. Fiz.* 41, 2571 (1971) [*Sov. Phys. Tech. Phys.* 16, 2041 (1972)].

Translated by J. G. Adashko

Distinguishing features of generation of the second harmonic of an electromagnetic wave in a magnetoactive plasma

N. S. Erokhin, S. S. Moiseev, and A. P. Shuklin

Kharkov State University

(Submitted 10 April 1980)

Zh. Eksp. Teor. Fiz. 79, 2152-2166 (December 1980)

Second-harmonic generation upon incidence of an electromagnetic wave on a weakly inhomogeneous plasma is investigated under conditions when the plasma density gradient is perpendicular to the external magnetic field. The efficiency of energy conversion into the second harmonic is calculated and the dependence of the effect on the polarization of the wave incident on the plasma is indicated.

PACS numbers: 42.65.Cq

INTRODUCTION

It was shown earlier¹ that when a p -polarized electromagnetic wave is incident on a weakly inhomogeneous cold isotropic plasma, a second harmonic is observed in the reflected signal. This effect occurs only in an inhomogeneous plasma because of the following circumstances. First, in an inhomogeneous isotropic plasma the nonlinear current induced at double the frequency by the incident wave is not purely longitudinal, but has a transverse component proportional to the gradient of the plasma density. Second, in an inhomogeneous isotropic plasma there exists near the critical-density surface a unique high- Q resonator in which the amplitude of the first field harmonic reaches anomalously high values. Owing to the small thickness of this resonator (compared with the wavelength of the second harmonic), the spectrum of the spatial harmonics of the nonlinear current broadens and occupies the region of the second-harmonic phase velocities, and it is this which leads to effective generation of the double-frequency wave from the region of the critical plasma density.

Second-harmonic generation has by now been investigated by many workers (see, e.g., Refs. 2-5), the main premises of the theory have been confirmed, and

the effect is being used in plasma diagnostics. Since the plasma contains frequently quasistationary magnetic field (either produced by extraneous sources or spontaneously generated in the plasma as a result of the development of various instabilities⁶⁻¹⁰), a need arises for the study of the effect of the magnetic field on the generation of the second harmonic of the electromagnetic wave. This is important both for a correct interpretation of the experimental data and to determine the conditions under which the effect can be used, as well as the distinguishing features of the second-harmonic generation in a magnetoactive plasma.

The features of second-harmonic generation in a magnetoactive plasma are connected mainly with the change of the dispersion of the electromagnetic waves. Thus, in a magnetoactive plasma it is necessary to take into account the possibility of synchronism (coincidence of the refractive indices) between the harmonics, even if the thermal corrections to the wave dispersion are negligibly small. An important role is played by the presence of points of intersection of the electromagnetic-oscillation modes, as well as the agreement between the location of the singularities of the first harmonic and of its refractive index. It will be shown below that in a magnetoactive plasma a singularity of the second-harmonic field can be located in the region of propaga-